International Journal of Biochemistry and Cell Biology 112 (2019) 61–71

Contents lists available at ScienceDirect

International Journal of Biochemistry and Cell Biology

journal homepage: www.elsevier.com/locate/biocel

MiR-9 promotes synovial sarcoma cell migration and invasion by directly targeting CDH1

Xue-Zheng Xu, Xian-An Li, Yi Luo, Jian-Fan Liu, Hong-Wei Wu, Gang Huang*

Department of Orthopedics, Hunan Cancer Hospital and the Affiliated Cancer Hospital of Xiangya School of Medicine, Central South University, Changsha, 410013, PR China

ARTICLE INFO

Keywords:
Synovial sarcoma
MiR-9
Epithelial mesenchymal transition
E-cadherin
MAPK/ERK
Wnt/β-catenin

ABSTRACT

Background: Invasion and metastasis of synovial sarcoma is the leading cause of death in patients. Epithelial mesenchymal transition (EMT) accelerates tumor cell invasion and metastasis. MiR-9 promotes tumor metastasis by inducing EMT. However, the role of miR-9 in synovial sarcoma is still not clear.

Methods: Overexpression or knockdown of miR-9 in human synovial sarcoma (HSS) cell lines was carried out by miR-9 mimics or miR-9 inhibitors transfection. Cell proliferation, apoptosis, migration and invasion were detected using MTS and colony formation assays, flow cytometry, wound healing and transwell assays, respectively. Luciferase reporter assay was applied to study the interaction between miR-9 and CDH1. Nude mice xenograft model was established, and immunohistochemistry staining assessed Ki-67 level. The related mRNA and protein expression levels were evaluated by qRT-PCR and Western blotting.

Results: The bioinformatics analyses and luciferase reporter assay showed that miR-9 can target CDH1 3′-UTR. Moreover, miR-9 could induce EMT of HSS cells via targeting CDH1. The negative regulation of miR-9 on CDH1 expression was also confirmed in a mouse xenograft model of synovial sarcoma. Furthermore, miR-9 was observed to induce HSS cell proliferation, migration and invasion and inhibit apoptosis. MAPK/ERK and Wnt/β-catenin signal pathways were activated by the miR-9 overexpression in HSS cells, and then further enhancing tumorigenesis of HSS, which was further confirmed in the mouse model.

Conclusion: MiR-9 induces EMT by targeting CDH1, and activates MAPK/ERK and Wnt/β-catenin signal pathways, thus promoting HSS tumorigenesis.

1. Introduction

Synovial sarcoma (SS) is a kind of soft tissue malignant sarcoma that features uncertain tissueorigins. It accounts for about 5–10% of soft tissue sarcomas, and may strike all age groups of people, yet with middle-aged and young people between 15 and 35 years old holding the largest part (Krieg et al., 2011). Although synovial sarcoma has a high malignancy and yearly increasing incidence, the comprehensive treatment dominated by surgery and supplemented by radiotherapy and chemotherapy in recent years has to a certain extent improved the survival rate of patients. However, the 5-year survival rate is still only about 50% (Stacchiotti and Van Tine, 2018). Synovial sarcoma has a high rate of metastasis with the metastasis rate 2 years after surgery being up to 40% (Krieg et al., 2011; Stacchiotti and Van Tine, 2018). Therefore, to explore the molecular biological mechanisms that affect the metastasis and recurrence of synovial sarcoma is of great significance to evaluate the prognosis of patients and molecular targeted therapy.

Epithelial mesenchymal transition (EMT) refers to the process that the epithelia with polarity in some special physiological or pathological conditions lose their polarity and are converted into the interstitial cells that have mobility and can move freely between cellular matrixes (Nistico et al., 2012). EMT is closely related to tumor invasion and metastasis, and is one of the hotspots in the research of tumor metastasis mechanism in recent years. E-cadherin (also known as CDH1), N-cadherin and β-catenin are the common markers to determine the occurrence of EMT. These proteins are involved in cell differentiation and play an important role in maintaining cell morphology and regulating intercellular adhesion (Nistico et al., 2012; Zeisberg and Neilson, 2009). E-cadherin, an EMT-related protein, is involved in epithelial adhesion and desmosomal junction, which play an important role in maintaining cell morphology, cell motility and cell adhesion (Zeisberg

* Corresponding author at: Department of Orthopedics, Hunan Cancer Hospital and the Affiliated Cancer Hospital of Xiangya School of Medicine, Central South University, No.283, Tongzipo Road, Yuelu District, Changsha, 410013, Hunan Province, PR China.
E-mail address: huanggang401@163.com (G. Huang).

https://doi.org/10.1016/j.biocel.2019.04.001
Received 13 November 2018; Received in revised form 18 March 2019; Accepted 4 April 2019
Available online 05 April 2019
1357-2725/

and Neilson, 2009; Onder et al., 2008). CDH1 is an important intercellular adhesion molecule, with the role of inhibiting tumor metastasis (Petrova et al., 2016). The adhesion function of cadherin/catenin complex depends on its integrity, so any change of its component members in quality and amount may lead to complex dysfunction, thus resulting into cell detachment, invasion and metastasis. The absence of CDH1 is an important landmark change of EMT, and a prerequisite for epithelial tumor cells possessing invasion abilities. (Saito et al. (2004) found that the down-regulation of CDH1 was related to the loss or absence of synovial sarcoma-like epithelial differentiation. The loss of CDH1 allows intercellular adhesion to loosen and thus makes cells migrate more easily to result in distant metastases. In epithelial tumors, CDH1 gene has become a new tumor suppressor gene, so that its mutation and loss are one of the key molecular events in cancer progression and metastasis.

MicroRNA is a kind of small, non-coding RNA containing about 22 nucleotide sequences and widely spreading in animals, plants and some viruses (Ma, 2016). Its main functions include silencing RNA and conducting post-transcriptional regulation of gene expression. Recent studies showed that miRNAs played important roles in tumorigenesis and metastasis, which provided a new idea for the prevention and treatment of tumor recurrence and metastasis (Jiang et al., 2015; Colden et al., 2017). (Sarver et al. (2010) suggested that the specific expression of miR-183 family might be associated with synovial sarcoma metastasis and recurrence, and the miR-183 family might be a potential carcinogenic factor during the formation of synovial sarcoma. As a member of the miRNA family, miR-9 has been proven associated with the development, growth, and metastasis of multiple tumors. For example, in studying the bronchial squamous epithelium carcinogenesis, (Mascaux et al. (2009) found that miR-9 had varied expressions at different stages of lesion. (Luo et al. (2009) confirmed with miRNA microarray and qRT-PCR that miR-9 had a low expression in gastric cancer tissues and SGC7901 cell line. (Yanaihara et al. (2016) discovered that miR-9 was overly expressed in ovarian clear cell carcinoma, which influenced tumor metastasis by inducing epithelial-mesenchymal transition with targeting CDH1. In addition, miR-9 has been shown to be significantly up-regulated in synovial sarcomas (over 30 times) (Yu et al., 2016), but the role of miR-9 in synovial sarcoma is still unclear. This study proposed that miR-9 regulates the EMT of synovial sarcoma cells by directly binding to CDH1, thus regulating the incidence and metastasis of synovial sarcomas.

2. Materials and methods

2.1. Cell culture

The human synovial sarcoma (HSS) cell lines SW982 and HS-SY-II (ATCC; USA) were cultured in Dulbecco's modified Eagle's medium (DMEM; Gibco, USA) supplemented with 10% fetal bovine serum(FBS; Sigma-Aldrich, St. Louis, MO, USA) at 37 °C with 5% $CO_2$and 100% humidity.

2.2. Cell transfection

MiR-9 mimics (5′-UCUUUGGUUAUCUAGCUGUAUGA-3′) and inhibitor (5′-UCAUACAGCUAGAUAACCAAAGA-3′) were purchased from GenePharma (Shanghai, China). Overexpression or knockdown of miR-9 was carried out by transfection with the miR-9 mimics or miR-9 inhibitors, respectively. The cells were plated in 6-well plates for 24 h and then transfected for 48 h with the miR-9 mimics or miR-9 inhibitors by using Lipofectamine 2000 (Thermo Fisher Scientific, USA) according to the manufacturer's instruction. CDH1 gene was cloned into pcDNA3.1 vector. For CDH1 overexpression, HSS cells were transfected with pcDNA3.1 plasmid encoding the CDH1 (pcDNA3.1-CDH1) by using Lipofectamine 2000 (Thermo Fisher Scientific, USA) according to the manufacturer's instruction.

2.3. MTS cell proliferation assay

Cell proliferation of HSS cells was detected using MTS cell proliferation colorimetric assay kit (BioVision, USA). The transfected cells were cultured onto 96-well plates with 200 μL of growth medium. After culturing for 48 h, 20 μL/well MTS Reagent was added into each well. After 4 h incubation at 37 °C, the absorbance at 490 nm was detected with a microplate reader (BioTek, USA).

2.4. Colony formation assay

HSS cells were plated in 6-well plates and cultured for 2 weeks. The plates were then washed with phosphate buffered saline (PBS) for twice, and cells were fixed with methanol-acetic acid. Cells were then stained with 0.5% cristal violet. The number of colonies was counted under a microscope (Olympus, Japan).

2.5. Luciferase reporter assay

We performed luciferase reporter assay on HSS cell lines. The CDH1 3′ untranslated region (UTR) clones (wild type3′UTR and mutant 3′UTR) were custom designed and synthesized by Sangon Biotech (Shanghai, China). CDH1 3′UTR was individually cloned into pGL4 luciferase reporter plasmid (Promega, USA). Then, cells were co-transfected with pGL4-CDH1 or control reporter pGL4 reporter plasmids and miR-9 mimics or inhibitor using Lipofectamine™ 2000 Reagent (Invitrogen). After culturing for 48 h, the relative luciferase activity was measured using Dual-Glow Luciferase Assay kit (Promega, USA) and a GloMax-Multi Detection System (Promega, USA).

2.6. Flow cytometry analysis of cell apoptosis

Apoptotic cells were identified using the Propidium Iodide (PI) Flow Cytometry Kit (abcam, USA) and FITC Annexin V Apoptosis Detection Kit I (BD, USA) according to the manufacturer's instructions. HSS cells were collected, washed twice with cold PBS and resuspended in 1 × binding buffer. For the cell apoptosis analysis, the cells were stained with 5 μL Annexin V-FITC for 15 min and then 5 μL PI for 10 min in the dark at room temperature. The cells were examined using Beckman cytoflex flow cytometry (Beckman, USA). The Cytexpert Software was applied for the flow cytometry data analysis. The statistical apoptotic rate was the sum of early apoptosis (Annexin V-$FITC^+PI^-$) and late apoptosis (Annexin V-$FITC^+PI^+$).

2.7. Wound healing assay

Cells (5×10^4) were seeded in 24-well plates and incubated at 37 °C. The confluent cells were scratched with a 200 μL pipette tip and photographed using an inverted microscope (IX71; Olympus, Center Valley, PA, USA). After 24 h incubation, plates were washed with fresh medium to remove non-adherent cells and then photographed using an inverted microscope (IX71; Olympus, Center Valley, PA, USA). Images were analyzed by ImageJ software (Wayne Rasband, USA). The extent of wound healing was determined by the ratio the area of the initial scratched area minus the area after 24 h to the initial scratched area.

2.8. Transwell assay

Cell migration assay was performed using a Transwell system (24-wells, 8 μm pore size with poly-carbonate membrane; SPL, Gyeonggi-do, Korea) according to the manufacturer's instructions. Briefly, post-transfected cells were trypsinized, and 1×10^5 cells were seeded into the upper chamber with serum free opti-MEM media. The low chamber was filled with 800 μL medium containing 10% FBS as a chemoattractant. After incubation for 48 h, cells on the lower side of the filter were fixed in 3.8% formaldehyde for 20 min and stained with 0.1%

crystal violet solution. The number of cells in five randomly selected fields was counted under a light microscope and analyzed statistically. For the invasion assay, the upper chamber was coated with extracellular matrix (BD Biosciences, Bedford, MA, USA), a soluble basement membrane matrix. The rest of the assay was performed as the migration assay.

2.9. Tumorigenesis and metastasis assays

The animal experiments were approved by the Ethic Committee of the Hunan Cancer Hospital. 21 six-week-old male BALB/c nude (nu/nu) mice were purchased from SJA Laboratory Animal Co., Ltd (Hunan, China). 400 μL of cells suspension (about 1×10^7) in PBS were subcutaneously injected into the nude mice. The mice were randomly divided into three groups and treated with: 1) SW982 cells transfected with miR- NC (NC group) 2) SW982 cells transfected with miR-9 mimics (miR-9 mimics group); 3) SW982 cells transfected with miR-9 inhibitor (miR-9 inhibitor group). After 21 days' cultivation, tumor sizes were measured every three days with electronic caliper. Tumor volume (V) was calculated by the formula: $V = 0.5 \times \text{length} \times \text{width}^2$. All mice were sacrificed at day 21 after treatments. Tumor samples were collected and weighed for all groups. For metastasis assay, cells were inoculated into the tail vein of nude mice, 30 days later, the mice were killed and the lungs of the mice were collected and paraffin embedded, consecutive sections (4 μm) were made and stained with hematoxylin-eosin staining.

2.10. Immunohistochemistry (IHC) staining

Xenograft tumor samples were collected and placed in formalin for immediate fixation. Sections were cut from paraffin blocks of formalin fixed tissue into 4 μm thick sections and mounted on charged slides. After deparaffinization, antigen retrieval, and blocking, the slides were incubated with mouse monoclonal anti-Ki-67 (1:100; Cell Signaling, USA) overnight at 4 °C. The sections were counterstained with Mayer's hematoxylin. The sections were then observed under a microscope.

2.11. RNA extraction and qRT-PCR

qRT-PCR was performed according to the MIQE guidelines (Bustin et al., 2009). RNA was isolated from HSS cells and xenograft tumor samples with TRIzol reagent (Invitrogen, USA) and RNeasy Plus Micro Kit (QIAGEN, USA) according to the manufacturer's instructions. RNA quality and quantity were assessed with agarose gel electrophoresis and A_{260}/A_{280} ratio with spectrophotometer (Nano Drop Technologies, Inc, Rockland, DE). The A_{260}/A_{280} ratios for all RNA preparations were about 1.8 ~ 2.0. Then, reverse transcription was conducted to synthesize the cDNA by utilizing the SuperScript®IV First-Strand Synthesis System (Invitrogen, USA). qRT-PCR was performed in Applied Biosystems 7500 Real Time PCR System (Applied Biosystems, USA), using 20 ng template in 25 μL reaction volume with 2 × Power SYBR® Green PCR Master Mix (Invitrogen, USA) and gene specific primer pairs for miR-9 (Forward: 5′-GCGCGTCTTTGGTTATCTAGCT-3′; Stem loop RT primer: 5′-GTCGTATCCAGTGCAGGGTCCGAGGTATTCGCACTGGATAC GACTCATAC-3′), human CDH1 (Forward: 5′-TCACATCCTACACTGCC CAG-3′; Reverse: 5′-AGTGTCCCTGTTCCAGTAGC-3′), mouse CDH1 (Forward: 5′-GTCTCCTCATGGCTTT GC-3′; Reverse: 5′-CTTTAGATGC CGCTTCAC-3′), β-catenin (Forward: 5′-AGGCTGCAGTTATGGTC CAT-3′; Reverse: 5′-AAGCATTTTCACCAGGGCAG-3′), ERK (Forward: 5′-CTGCTCAACACCACCTGTGA-3′; Reverse: 5′-GTCAGCATTTGGGAAC AGCC-3′), β-actin (Forward: 5′-GCAGGAGTACGATGAGTCCG-3′; Reverse: 5′-ACGCAGCTCAGTAACAGTCC-3′) and U6 (Forward: 5′-CTCGC TTCGGCAGCACA-3′; Reverse: 5′-AACGCTTCACGAATTTGCGT-3′) in HSS cell lines and xenograft tumor homogenates. Amplification conditions were as follows: 95 °C for 10 min followed by 45 cycles consisting of 95 °C for 15 s, 58 °C for 30 s and 68 °C for 60 s. The gene expression levels for all samples were normalized to U6 or β-actin expression using the comparative Ct method. All data are displayed as the mean ± SD of three independent experiments.

2.12. Western blot analysis

Xenograft tumor homogenates and HSS cells were harvested and lysed in the RIPA buffer (Sigma-Aldrich, USA).Protein concentrations were determined using the BCA proteinassay kit (Thermo Fisher Scientific, USA). Proteins (30 μg) were separated by 10% SDS-PAGE and transferred onto a nitrocellulose membrane. After blocking with BSA, the membranes were then incubated with primary antibodies against CDH1, MMP-2, MMP-9, N-cadherin, Vimentin, Fibronectin, β-catenin, ERK, phosphorylated ERK (p-ERK), and GAPDH (Abcam, USA). GAPDH was loaded as an internal reference. Bands were then treated with the goat anti-rabbit IgG-HRP secondary antibody (1:2000; Abcam, USA). Bands were developed using chemiluminescence substance (Thermo Scientific, USA).

2.13. Statistical analysis

Data were analyzed with Prism 5.0 (GraphPad Software, USA). All experiments were performed in triplicates and data were expressed as the means ± standard deviation (SD). Student's *t*-test (two tailed) and one-way analysis of variance (ANOVA) followed by Dunnett's test were applied for two or multiple comparison, respectively. $P < 0.05$ was considered significantly different.

3. Results

3.1. MiR-9 inhibits the CDH1 expression by targeting the 3′ untranslated region

In order to investigate the relationship between miR-9 and CDH1, overexpression or knockdown of miR-9 was carried out by transfection with the miR-9 mimics or miR-9 inhibitor, respectively. As shown in Fig. 1A, the expression of miR-9 was significantly up-regulated when transfected with miR-9 mimics, while the expression was dramatically down-regulated by the transfection of miR-9 inhibitor in both SW982 and HS-SY-II cells ($p < 0.05$, versus the NC group) (Fig. 1A). In addition, the expression of CDH1 was significantly down-regulated when the miR-9 was up-regulated, while that was dramatically up-regulated when the miR-9 was down-regulated ($p < 0.05$, versus the NC group) (Fig. 1B). This indicates that miR-9 may negatively regulate the expression of CDH1 in HSS cell lines. The bioinformatic analysis showed that CDH1 is a potential target for miR-9 (Fig. 1C). To further determine whether miR-9 targets CDH1, we performed luciferase reporter assay using wild type 3′UTR and mutant 3′UTR of CDH1. In MUT CDH1 3′UTR, the miR-9 binding sequence on 3′UTR of CDH1 was mutated. The HSS cells with either WT CDH1 3′UTR or MUT CDH13′UTR were treated with either miR-9 mimics, miR-9 inhibitors or NC, and relative luciferase activities were measured. We found that miR-9 mimics could decrease relative luciferase activity in WT CDH1 3′UTR compared to the NC group, suggesting that miR-9 targets CDH1 3′UTR (Fig. 1D&E). Moreover, luciferase activity was no change in both SW982 (Fig. 1D) and HS-SY-II (Fig. 1E) cells co-transfected with miR-9 mimics and the plasmid of MUT CDH1 3′UTR, further confirming that miR-9 targets CDH1 3′UTR.

3.2. MiR-9 induces EMT of HSS cells via targeting CDH1

Given the critical role of CDH1 in EMT, we further investigated the role of miR-9 in the EMT of HSS cells. The qRT-PCR results showed that the CDH1 was overexpressed by transfected with pcDNA3.1 plasmid encoding the CDH1 in both SW982 and HS-SY-II cell lines ($p < 0.01$, versus the pcDNA3.1 group) (Fig. 2A). Meanwhile, the same pattern

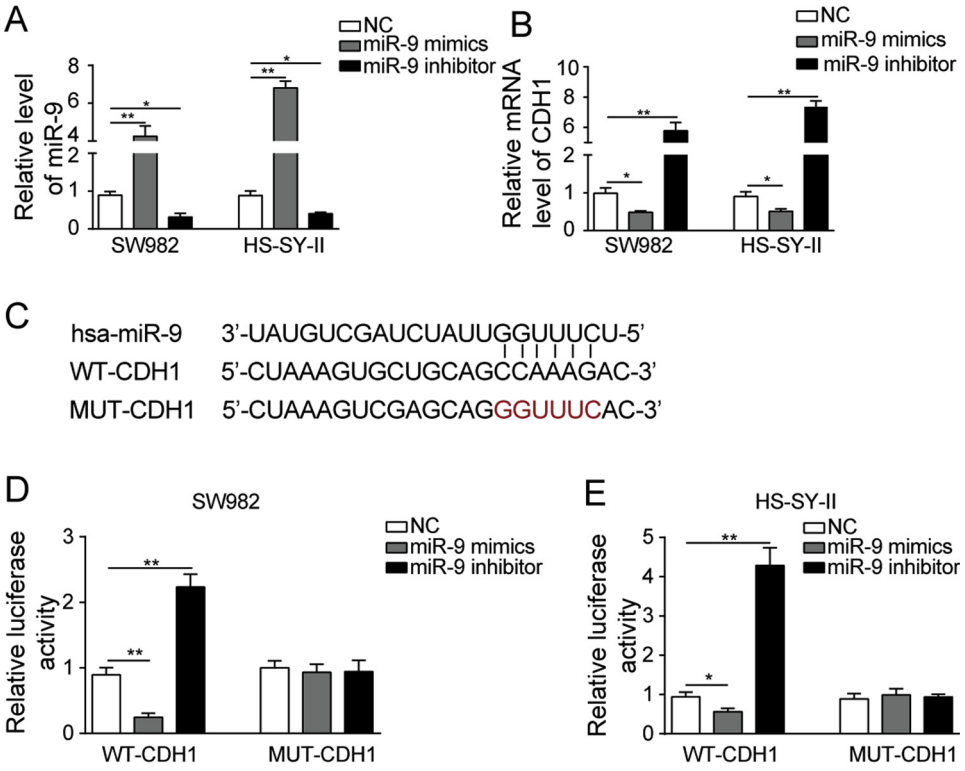

Fig. 1. MiR-9 inhibits the CDH1 expression by targeting CDH1 3′UTR. (A) Expression of miR-9 in SW982 and HS-SY-II cells when transfected with the miR-9 mimics or miR-9 inhibitor detected by qRT-PCR. (B) Expression of CDH1 in SW982 and HS-SY-II cells when transfected with the miR-9 mimics or miR-9 inhibitor detected by qRT-PCR. (C) Bioinformatics analyses of miR-9 potential binding sites on wild type 3′UTR and mutant 3′UTR of CDH1. (D&E) The HSS cells with either WT CDH1 3′UTR or MUT CDH1 3′UTR were treated with either miR-9 mimics, miR-9 inhibitor or negative control miRNA (NC), and relative luciferase activities were measured by luciferase reporter assayin both SW982 (D) and HS-SY-II (E) cells. All the results were expressed as mean ± SD (n = 3). ANOVA followed by Dunnett's test was applied for multiple comparison. *$p < 0.05$ and **$p < 0.01$.

was observed by the Western blot analysis (Fig. 2B&C). In addition, the expression of EMT related proteins were further investigated. As shown in Fig. 2D&E the expression of CDH1 was significantly down-regulated when the miR-9was overexpressed, while it was up-regulated by the inhibition of miR-9. However, the EMT related proteins, including MMP-2, MMP-9, N-cadherin, Vimentin and Fibronectin were significantly down-regulated when the miR-9 was knocked down, while those were significantly up-regulated when the miR-9 was overexpressed, which could be reversed by the overexpression of CDH1 ($p < 0.05$, versus the NC group; Fig. 2D&E). All these results indicate that miR-9 can induce EMT of HSS cells via targeting CDH1.

3.3. MiR-9 induces HSS cell migration and invasion via targeting CDH1

Whether miR-9 is involved in HSS cells migration and invasion was further investigated. The wound healing assay (Fig. 3A&B) showed that the migration of HSS cells was inhibited by miR-9 knockdown ($p < 0.01$, versus the NC group), while that was enhanced by miR-9 overexpression ($p < 0.05$, versus the NC group), which was reversed by CDH1 overexpression ($p < 0.05$, versus the miR-9 mimics group).The enhancement of cell migration by miR-9 overexpression in HSS cells was also proved by transwell migration assay (Fig. 3C&D). The transwell invasion assay (Fig. 3E&F) showed that the cell invasion abilities of HSS cells were also significantly increased by miR-9 overexpression comparison to the NC group ($p < 0.05$). All these results indicate that miR-9 can induce HSS cell migration and invasion via targeting CDH1.

3.4. MiR-9 stimulates proliferation and inhibits apoptosis of HSS cells

We further investigate the effect of miR-9 on HSS cell proliferation and apoptosis. As shown in Fig. 4A, the proliferation ability was inhibited by miR-9 knockdown in HSS cells ($p < 0.05$, versus the NC group), while that was enhanced by miR-9 overexpressed ($p < 0.01$, versus the NC group), which was reversed by CDH1 overexpression ($p < 0.05$, versus the miR-9 mimics group) (Fig. 4A). Moreover, the flow cytometry (Fig. 4B&C) revealed a significantly higher percentage of apoptotic cells in both HSS cell lines when the miR-9 was knocked down ($p < 0.01$, versus the NC group), while the apoptotic rate was down-regulated when the miR-9 was overexpressed ($p < 0.05$, versus the NC group), which was moderately reversed by CDH1 overexpression ($p < 0.01$, versus the miR-9 mimics group). Additionally, these effects were further confirmed by the colony formation assay (Fig. 4D&E), in which overexpression of miR-9 promoted HSS cell proliferation, knockdown of miR-9 inhibited cell proliferation, and overexpression of CDH1 reversed the effect of miR-9 on the cell proliferation. All these indicate that miR-9 can stimulate proliferation and inhibit apoptosis of both SW982 and HS-SY-II cells.

3.5. MAPK/ERK and Wnt/β-catenin signal pathways involve in the miR-9 regulation of the HSS tumorigenesis.

To further investigate the molecular mechanism of the miR-9 regulation of the tumorigenesis of HSS, additionally, the mRNA and protein expression levels of MAPK/ERK and Wnt/β-catenin signal pathway related molecules in HSS cells were investigated. As shown in Fig. 5A&B, transfection of miR-9 mimics increased the mRNA levels of β-catenin and ERK ($p < 0.05$, versus the NC group), while the expression levels of those were inhibited by the transfection of miR-9 inhibitor ($p < 0.05$, versus the NC group). Furthermore, the protein expression levels (Fig. 5C&D) of β-catenin, ERK, and p-ERK in both of HSS cells was significantly down-regulated ($p < 0.05$, versus the NC group) when the miR-9 was knocked down. Additionally, the expressions of these proteins were significantly up-regulated when the miR-9 was overexpressed ($p < 0.05$, versus the NC group), which was moderately reversed by CDH1 overexpression ($p < 0.05$, versus the miR-9 mimics group). All these results indicate that miR-9 overexpression can activate MAPK/ERK and Wnt/β-catenin signal pathways, thus enhancing the HSS cell proliferation and inhibiting apoptosis.

3.6. MiR-9 induces the tumorigenesis of synovial sarcoma in mice

We next evaluated the influence of miR-9 on the tumorigenesis of synovial sarcoma in mouse model. The tumor sizes in miR-9 knockdown

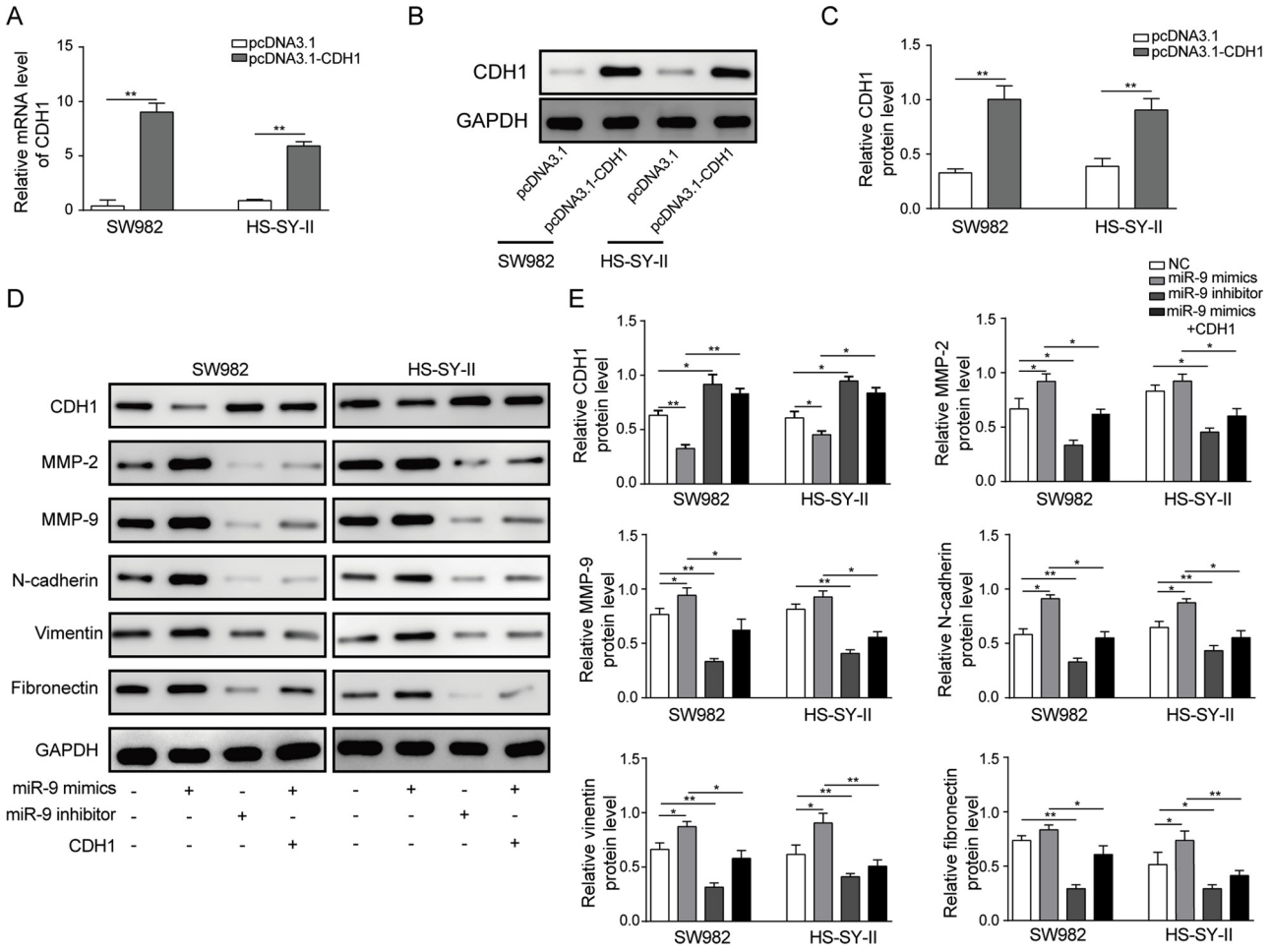

Fig. 2. MiR-9 induces EMT of HSS cells via targeting CDH1. (A&B) Expression of CDH1 in SW982 and HS-SY-II cells transfected with pcDNA3.1 plasmid encoding the CDH1 detected by qRT-PCR (A) and Western blot analysis (B). (C) Quantitative results of the Western blot analysis. (D) Western blot analysis of the expression of EMT related proteins in SW982 and HS-SY-II cells after transfection by the miR-9 mimics or miR-9 inhibitor. (E) Quantitative results of the Western blot analysis of EMT related proteins. All the results were expressed as mean ± SD (n = 3). Student's *t*-test (two tailed) and ANOVA followed by Dunnett's test were applied for two or multiple comparison, respectively. *p < 0.05 and **p < 0.01.

mice were significantly smaller than those from NC group ($p < 0.05$), while the tumor sizes were dramatically increased by miR-9 overexpression ($p < 0.01$, versus the NC group; Fig. 6A&B). A same pattern was observed for the weights of tumors harvested from mice at the end of experiments (Fig. 6C). Then, in the HE staining results (Fig. 6D), nuclear mitosis is enhanced and necrosis was observed in the miR-9 overexpressed tumor sections when compared with NC group samples, while the reversed pattern was observed in the miR-9 knockdown group. In addition, the IHC analysis (Fig. 6D&E) of tumor sections showed that more Ki-67 positive-cells were observed in the miR-9 overexpression group ($p < 0.0.1$, versus the NC group), while Ki-67 positive-cells were decreased in the miR-9 knockdown group ($p < 0.05$, versus the NC group), which indicates that miR-9 promotes the tumor cell proliferation. To further evaluate the effect of miR-9 on lung metastasis, we injected HSS cells into nude mice in the tail vein. As shown in Fig. 6F&G, mice with miR-9 overexpression had grossly apparent lung metastases, but much less metastasis was observed in mice with miR-9 inhibition. The HE staining for lung tissues exhibited a same pattern (Fig. 6F&G), indicating that miR-9 promotes lung metastasis of synovial sarcoma.

3.7. MiR-9 stimulates EMT and activates MAPK/ERK and Wnt/β-catenin signal pathways in a mouse xenograft model of synovial sarcoma

The miR-9 expression levels were determined by qRT-PCR in a mouse xenograft model of synovial sarcoma. As shown in Fig. 7A, miR-9 expression was significantly decreased in the miR-9 knockdown mice, and dramatically increased in the miR-9 overexpression mice when compared with the NC group ($p < 0.05$). Consistently, the qRT-PCR results showed that the CDH1 mRNA expression level was negatively regulated by miR-9 (Fig. 7B). Meanwhile, the EMT, and MAPK/ERK and Wnt/β-catenin signal pathways related proteins in SS tumor samples were detected by Western blotting (Fig. 7C). As shown in Fig. 7C&D, CDH1 was decreased, N-cadherin and Vimetin were increased in the miR-9 overexpression tumor sample when compared with the NC group, while CDH1 was increased, N-cadherin and Vimetin were decreased in the miR-9 knockdown sample. Moreover, the protein expression levels of β-catenin, ERK, and p-ERK in SS tumor samples (Fig. 7C&D) were significantly down-regulated ($p < 0.05$, versus the NC group) when the miR-9 was knocked down. Additionally, the expressions of these proteins were significantly up-regulated ($p < 0.05$, versus the NC group) when the miR-9 was overexpressed. These results further confirm that miR-9 can target CDH1 in the mouse model thus stimulating EMT, and enhance the tumorigenesis of HSS in mice via activating MAPK/ERK and Wnt/β-catenin signaling pathways.

4. Discussion

One of the most important features of malignant tumor is its ability of invasion and metastasis, which is the leading cause of death in

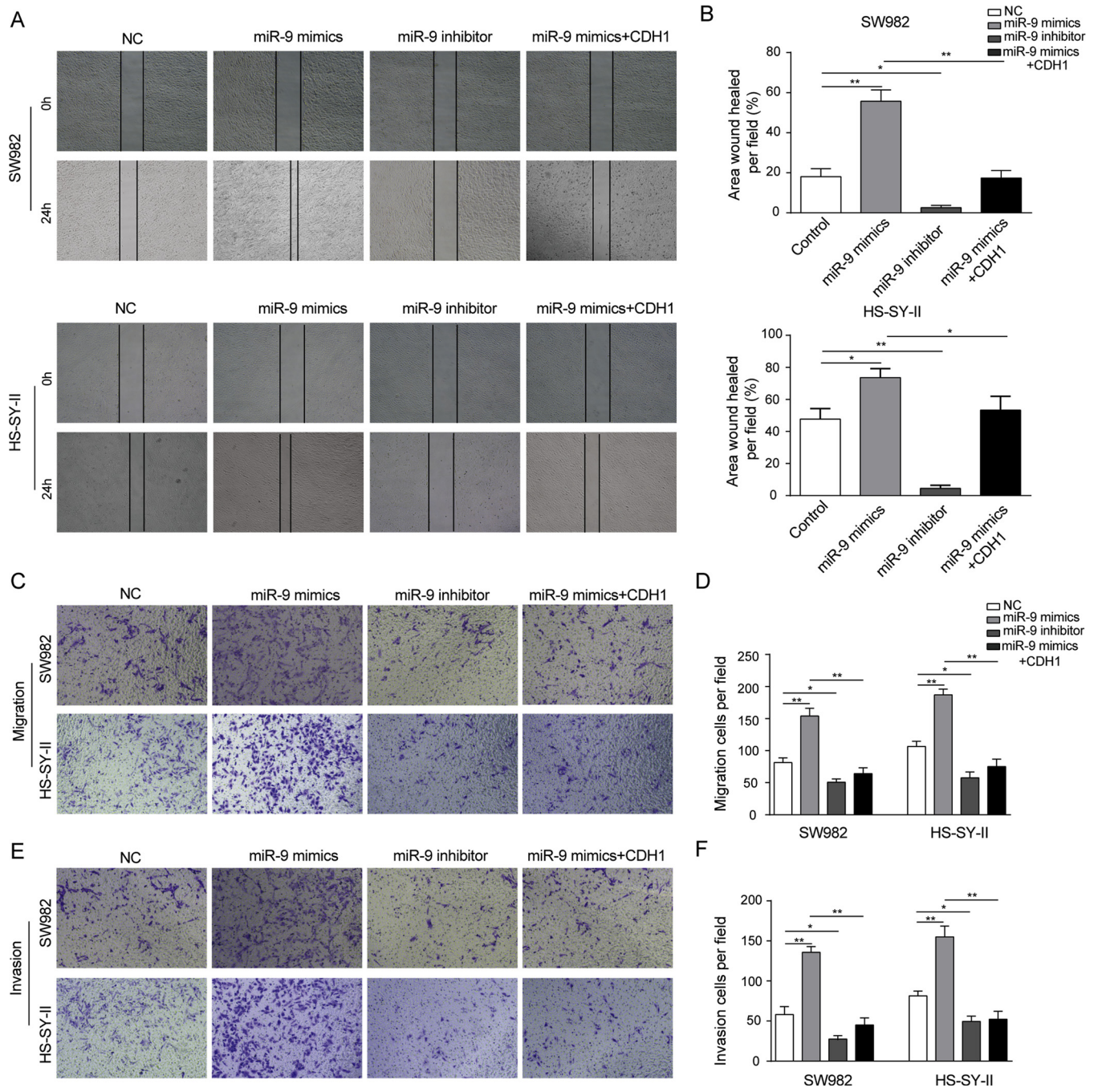

Fig. 3. MiR-9 induces HSS cell migration and invasion via targeting CDH1. (A) HSS cell migration abilities detected by wound healing assay. (B) Quantification of the wound area determined using an inverted microscope. (C) HSS cell migration abilities detected by transwell migration assay. (D) The cells migration rate (cell count per filed) among different groups were quantified. (E) HSS cell invasion abilities detected by transwell invasion assay. (F) The cells invasion rate (cell count per filed) among different groups were quantified. All the results were expressed as mean ± SD (n = 3). ANOVA followed by Dunnett's test was applied for multiple comparison. *$p < 0.05$ and **$p < 0.01$.

patients with synovial sarcoma. Although the survival rate has witnessed improvement, metastasis is still an important cause of death in patients with synovial sarcoma. Therefore, looking for an effective therapeutic schedule to control tumor metastasis will be the focus and difficulty of synovial sarcoma treatment.

Currently, it has been clear that the potential of tumor invasion and metastasis depends on the interaction of internal environmental factors, among which EMT is one of the main factors of tumor cell invasion and metastasis (Heerboth et al., 2015). The occurrence of EMT mainly depends on the expression of CDH1 and the change in its stability (Onder et al., 2008). CDH1 acts as an important intercellular adhesion molecule, and its expression is negatively correlated to tumors' invasion and metastasis abilities. The expression of CDH1 is present in many human tumors, such as colorectal cancer, gastric cancer, breast cancer, esophageal cancer, liver cancer, renal cancer, and prostate cancer (Wicki and Christofori, 2016). CDH1 in these human malignant tumor cells tends to be lowly expressed, and overexpression of CDH1 inhibits tumor invasion and metastasis. Consistently, in present study, the down-regulated expression of CDH1 would induce the HSS cell migration and invasion, which indicates that the reduced CDH1 level may lower the adhesion ability of cells, thereby promoting tumor invasion and metastasis.

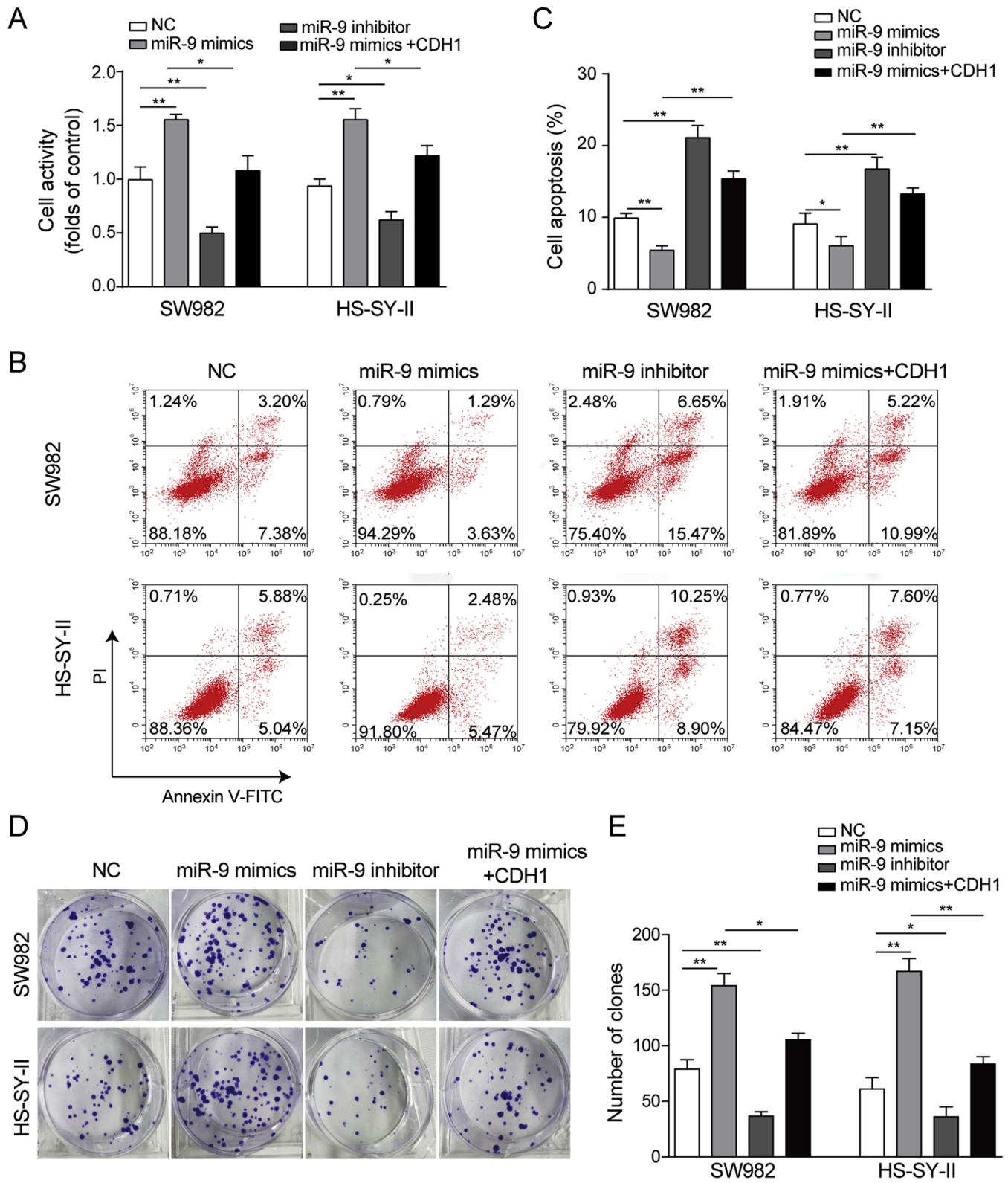

Fig. 4. MiR-9 promotes proliferation and inhibits apoptosis of HSS cells. (A) HSS cell proliferation abilities detected by MTS cell proliferation assay among different groups. (B) Apoptotic cells were identified using the Propidium Iodide (PI) and FITC Annexin V using flow cytometry. (C) Apoptosis cells were quantified. (D) Effect of miR-9 on the HSS cell proliferation tested by the colony formation assay. (E) The amount of colony formation was counted. All the results were expressed as mean ± SD (n = 3). ANOVA followed by Dunnett's test was applied for multiple comparison. *$p < 0.05$ and **$p < 0.01$.

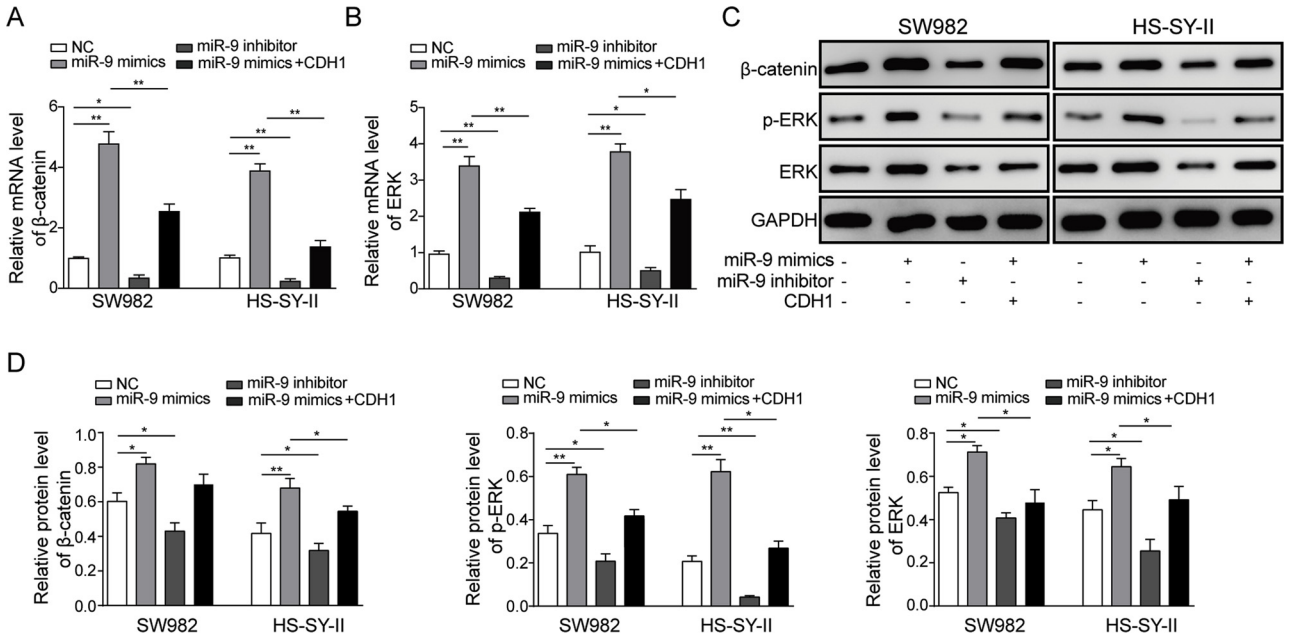

Fig. 5. MiR-9 can activate MAPK/ERK and Wnt/β-catenin signaling pathways in HSS cells. The mRNA expression levels of β-catenin (A) and ERK (B) in HSS cells when the miR-9 was knocked down or overexpressed or the CDH1 was overexpression detected by qRT-PCR. (C) Expression levels of MAPK/ERK and Wnt/β-catenin signal pathway related proteins in HSS cells when the miR-9 was knocked down or overexpressed or the CDH1 was overexpression detected by Western blotting. (D) Quantitative results of the Western blotting analysis. All the results were expressed as mean ± SD (n = 3). ANOVA followed by Dunnett's test was applied for multiple comparison. *$p < 0.05$ and **$p < 0.01$.

A variety of miRNA molecules have been reported to specifically affect the process of EMT, exerting great influences upon the invasion and migration abilities of tumor cells. For instance, when tumor cells undergo EMT, miR-205 and miR-200 therein will be down-regulated, thereby inhibiting the activity of ZEB family transcription factors, and further regulating the expression of EMT related proteins like CDH1 (Gregory et al., 2008). Meanwhile, some miRNA molecules can play a role in controlling the EMT process at different levels. For example, miR-141 can directly inhibit the expression of transforming growth factor-β (TGF-β), which is a key regulator of EMT (Huang et al., 2015). Research has shown that in the early stage of malignant breast cancer, the elevated level of miR-9 could promote the EMT of tumor cells, and enhance the growth of blood vessels, thus increasing the blood supply to tumors and promoting tumor growth and invasion (Gwak et al., 2014). It has been also reported that miR-9 was significantly up-regulated in laryngeal carcinoma and human laryngeal carcinoma cell line Hep-2, and the knockdown of miR-9 could inhibit Hep-2 cell proliferation (Lu et al., 2016). In addition, (Yu et al. (2016)) recently reported that of the 99 overexpressed miRNAs in synovial sarcoma, miR-9 had the highest fold changes (about 30 times), however, the specific role of miR-9 in HSS and related molecular mechanisms have not been reported. In this study, our bioinformatics analyses showed that CDH1 is a potential target for miR-9, and miR-9 may negatively regulate the expression of CDH1 in HSS cell lines. Furthermore, our luciferase reporter assay further showed that miR-9 decreased relative luciferase activity in WT CDH1 3′UTR with respect to the NC group, suggesting that miR-9 targets WT CDH1 3′UTR. Moreover, our qRT-PCR results showed that the expression of CDH1 was significantly down-regulated, and the EMT related proteins, including MMP-2, MMP-9, N-cadherin, Vimentin and Fibronectin were significantly up-regulated when the miR-9 was overexpressed. Meanwhile, the CDH1 mRNA expression level was negatively regulated by miR-9 in a mouse xenograft model of synovial sarcoma. Therefore, we conclude that miR-9 can induce EMT of HSS cells by targeting CDH1.

Since CDH1 expression is negatively correlated to tumors' invasion and metastasis abilities, as expected, we observed that the migration of HSS cells was enhanced by miR-9 overexpressed, which was reversed by CDH1 overexpression. This indicates that miR-9 can induce HSS cell migration and invasion via targeting CDH1. In 2017, (Han et al. (2017)) reported that miR-9 was up-regulated by TGF-β1 and involved in TGF-β1-induced lung cancer cell invasion and adhesion. Considering the regulating role of TGF-β in EMT, interestingly, (Qi et al. (2017)) proposed that TGF-β1 could promote the EMT process in HSS cells. Combined with our results, we speculated that TGF-β1 may promote the expression of miR-9, and further regulate the EMT process of HSS. Further studies are needed to validate this hypothesis in the future.

Researched have shown that a variety of signal transduction pathways involve in tumor EMT process, such as TGF-β, Mitogen-activated protein kinase (MAPK), Notch and Wnt signaling pathways (Zhang et al., 2016; Seoane and Gomis, 2017; Sheng et al., 2017; Tang et al., 2017). Wnt/β-catenin signaling pathway is also known as the classic Wnt pathway. Wnt gene is abnormally activated in tumors, inhibiting the phosphorylation of β-catenin by GSK3β/APC/Axin complex, thus reducing the phosphorylation degradation of β-catenin. Then, the cytosolic accumulated β-catenin will enter the nucleus to interact with nuclear transcription factor T lymphocyte factor (TCF)/lymphoid enhancer factor (LEF), thereby activating a number of downstream target genes for overexpression, such as cyclinD1 and c-myc (Gonzalez and Medici, 2014; Howard et al., 2011). During this process, β-catenin plays a key role. It may bind to the intracellular region of CDH1 to form β-catenin/CDH1 complex, and then connect with actin skeleton to weaken intercellular adhesion and induce tumor EMT process, thereby enhancing the invasion and metastasis of tumor cells. (Su et al. (2012)) reported that miR-200 could bind to the E-box motif in the promoter region of CDH1, inhibiting the transcription of CDH1 and promoting EMT. When CDH1 expression is abnormal, β-catenin enters nucleus from cytoplasm, activating Wnt signaling pathway. It has been reported that miR-9 could promote EMT in breast cancer via reducing CDH1 and increasing Vimentin levels, thus leading to the translocation of active β-catenin into the nucleus where it induced the transcription of oncogenes (Ma et al., 2010). Abnormally activated Wnt pathway can promote tumor formation, proliferation and migration. Consistently, we found that Wnt/β-catenin signaling pathway was activated by the miR-9 overexpression in HSS cells, and then further enhancing HSS cell

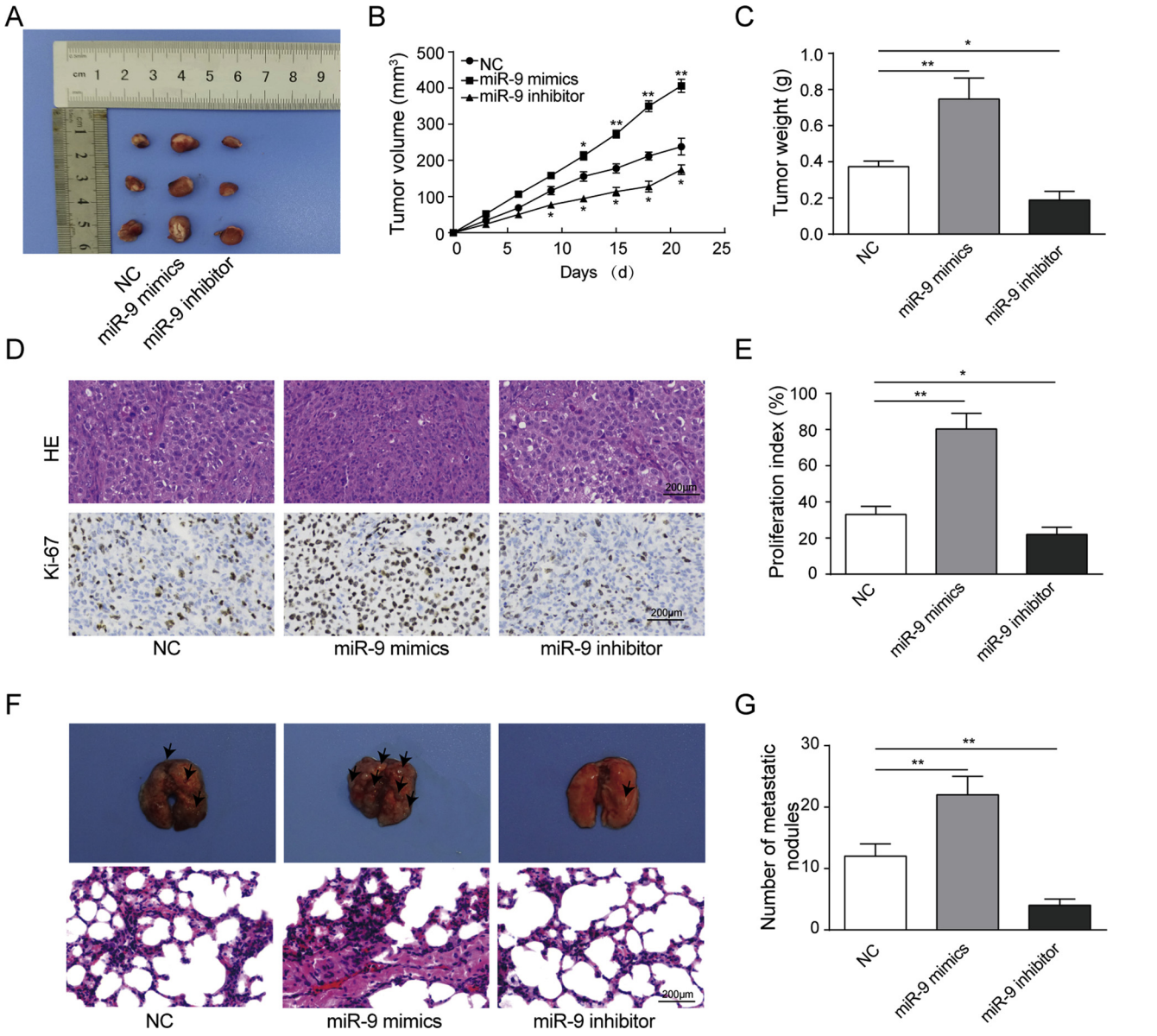

Fig. 6. MiR-9 induces the tumorigenesis of synovial sarcoma in mice. (A) Xenograft tumor samples were isolated from mice after 21 days' cultivation, and (B) the tumor sizes were measured every three days with electronic caliper. Tumor volume (V) was calculated by the formula: $V = 0.5 \times \text{length} \times \text{width}^2$. (C) Tumor samples were collected and weighed for all groups. (D) HE staining and IHC analysis of the tumor samples among different groups. Scale bar: 200 μm. (E) The tumor cell proliferation was quantified as the Ki-67 positive-cells. (F) Representative images of lung metastatic nodules. The lung metastases in nude mice (upper panel) and HE staining for lung tissues in nude mice (lower panel). (G) The number of metastatic nodules in the lung of nude mice. All the results were expressed as mean ± SD (n = 3). ANOVA followed by Dunnett's test was applied for multiple comparison. *$p < 0.05$ and ** $p < 0.01$.

proliferation and inhibiting apoptosis. Moreover, the protein expression levels of β-catenin in HSS tumor model were significantly up-regulated when the miR-9 was overexpressed.

MAPK is a kind of intracellular serine/threonine protein kinase (Gui et al., 2012). It is found that the vast majority of tumors have witnessed the abnormal activation of MAPK-related pathways. There are three MAPK signaling pathways widely studied, namely, JNK signaling pathway, p38 MAPK signaling pathway and RAS-RAF-MEK-ERK pathway, all of which participate in tumor EMT process. Making use of MEK acting on malignant gliomacells, (Guo et al. (2013)) confirmed that MEK phosphorylation level and ERK level were significantly reduced after oleanolic acid treatment. Additionally, the up-regulation of CDH1, the down-regulation of N-cadherin and Vimentin suggest that the MAPK/ERK signaling pathway is closely related to the EMT of glioblastoma epithelial cells. By overexpression of miR-9, (Xiong et al. (2018)) reported that phosphorylated ERK was altered to enhance the radio-sensitivity of lung cancer cells. In our study, the mRNA level of ERK and the protein levels of ERK and p-ERK in both HSS cells were significantly down-regulated when the miR-9 was knocked down. Additionally, the expressions of these proteins were significantly up-regulated when the miR-9 was overexpressed, which was moderately reversed by CDH1 overexpression. These indicate that miR-9 can also activate MAPK/ERK signal pathway, thus enhancing the HSS cell proliferation and inhibiting apoptosis. Meanwhile, the critical role of miR-9 in the tumorigenesis of HSS was further confirmed in our mouse model that miR-9 influences the tumorigenesis of HSS in mice via activating MAPK/ERK and Wnt/β-catenin signal pathways.

5. Conclusions

Taken together, miR-9 plays a critical role in the tumorigenesis of HSS via targeting CDH1. MiR-9 can induce EMT by targeting CDH1,

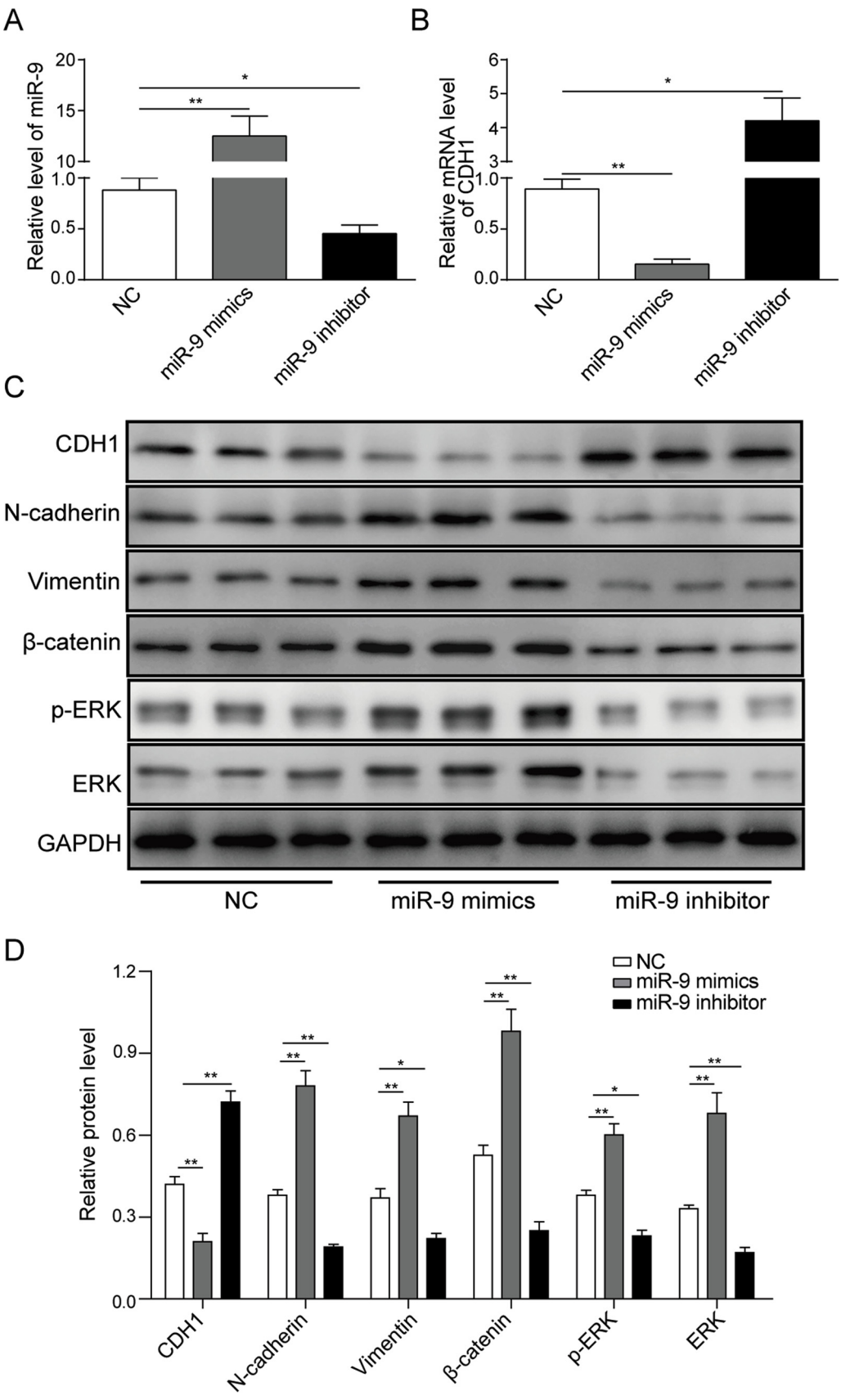

Fig. 7. MiR-9 stimulates EMT and activates MAPK/ERK and Wnt/β-catenin signaling pathways in a mouse xenograft model of synovial sarcoma. Xenograft tumor samples were isolated from mice after 21 days' cultivation. (A) MiR-9 expression levels in a mouse xenograft model of synovial sarcoma among different groups determined by qRT-PCR. (B) CDH1 expression levels in a mouse xenograft model of synovial sarcoma among different groups determined by qRT-PCR. (C) EMT and MAPK/ERK and Wnt/β-catenin signaling pathways related proteins in HSS tumor samples were detected by Western blotting. (D) The relative expression levels of corresponding proteins were quantified. All the results were expressed as mean ± SD (n = 3). ANOVA followed by Dunnett's test was applied for multiple comparison. *$p < 0.05$ and **$p < 0.01$.

thus promoting tumor invasion and metastasis. Furthermore, miR-9 was found to activate MAPK/ERK and Wnt/β-catenin signal pathways in HSS cells, thereby enhance the tumorigenesis of HSS in a mouse model. This study is conducive for us to better understanding the pathogenesis of HSS. MiR-9 may serve as a new and important molecular target for the treatment of synovial sarcoma.

Funding

This research did not receive any specific grant from funding agencies in the public, commercial, or not-for-profit sectors.

Conflict of interest

The authors declare that there are no conflict of interest.

Acknowledgements

We would like to give our sincere gratitude to the reviewers for their constructive comments.

Appendix A. Supplementary data

Supplementary material related to this article can be found, in the online version, at doi:https://doi.org/10.1016/j.biocel.2019.04.001.

References

Bustin, S.A., Benes, V., Garson, J.A., Hellemans, J., Huggett, J., Kubista, M., Mueller, R., Nolan, T., Pfaffl, M.W., Shipley, G.L., Vandesompele, J., Wittwer, C.T., 2009. The MIQE guidelines: minimum information for publication of quantitative real-time PCR experiments. Clin. Chem. 55, 611–622.

Colden, M., Dar, A.A., Saini, S., Dahiya, P.V., Shahryari, V., Yamamura, S., Tanaka, Y., Stein, G., Dahiya, R., Majid, S., 2017. MicroRNA-466 inhibits tumor growth and bone metastasis in prostate cancer by direct regulation of osteogenic transcription factor RUNX2. Cell Death Dis. 8, e2572.

Gonzalez, D.M., Medici, D., 2014. Signaling mechanisms of the epithelial-mesenchymal transition. Sci. Signal. 7, re8.

Gregory, P.A., Bert, A.G., Paterson, E.L., Barry, S.C., Tsykin, A., Farshid, G., Vadas, M.A., Khew-Goodall, Y., Goodall, G.J., 2008. The miR-200 family and miR-205 regulate epithelial to mesenchymal transition by targeting ZEB1 and SIP1. Nat. Cell Biol. 10, 593–601.

Gui, T., Sun, Y., Shimokado, A., Muragaki, Y., 2012. The roles of mitogen-activated protein kinase pathways in TGF-beta-Induced epithelial-mesenchymal transition. J. Signal Transduct. 2012, 289243.

Guo, G., Yao, W., Zhang, Q., Bo, Y., 2013. Oleanolic acid suppresses migration and invasion of malignant glioma cells by inactivating MAPK/ERK signaling pathway. PLoS One 8, e72079.

Gwak, J.M., Kim, H.J., Kim, E.J., Chung, Y.R., Yun, S., Seo, A.N., Lee, H.J., Park, S.Y., 2014. MicroRNA-9 is associated with epithelial-mesenchymal transition, breast cancer stem cell phenotype, and tumor progression in breast cancer. Breast Cancer Res. Treat. 147, 39–49.

Han, L., Wang, W., Ding, W., Zhang, L., 2017. MiR-9 is involved in TGF-beta1-induced lung cancer cell invasion and adhesion by targeting SOX7. J. Cell. Mol. Med. 21, 2000–2008.

Heerboth, S., Housman, G., Leary, M., Longacre, M., Byler, S., Lapinska, K., Willbanks, A., Sarkar, S., 2015. EMT and tumor metastasis. Clin. Transl. Med. 4, 6.

Howard, S., Deroo, T., Fujita, Y., Itasaki, N., 2011. A positive role of cadherin in Wnt/beta-catenin signalling during epithelial-mesenchymal transition. PLoS One 6, e23899.

Huang, Y., Tong, J., He, F., Yu, X., Fan, L., Hu, J., Tan, J., Chen, Z., 2015. miR-141 regulates TGF-beta1-induced epithelial-mesenchymal transition through repression of HIPK2 expression in renal tubular epithelial cells. Int. J. Mol. Med. 35, 311–318.

Jiang, C., Chen, X., Alattar, M., Wei, J., Liu, H., 2015. MicroRNAs in tumorigenesis, metastasis, diagnosis and prognosis of gastric cancer. Cancer Gene Ther. 22, 291–301.

Krieg, A.H., Hefti, F., Speth, B.M., Jundt, G., Guillou, L., Exner, U.G., von Hochstetter, A.R., Cserhati, M.D., Fuchs, B., Mouhsine, E., Kaelin, A., Klenke, F.M., Siebenrock, K.A., 2011. Synovial sarcomas usually metastasize after &5 years: a multicenter retrospective analysis with minimum follow-up of 10 years for survivors. Ann. Oncol. 22, 458–467.

Lu, E., Su, J., Zeng, W., Zhang, C., 2016. Enhanced miR-9 promotes laryngocarcinoma cell survival via down-regulating PTEN. Biomed. Pharmacother. 84, 608–613.

Luo, H., Zhang, H., Zhang, Z., Zhang, X., Ning, B., Guo, J., Nie, N., Liu, B., Wu, X., 2009. Down-regulated miR-9 and miR-433 in human gastric carcinoma. J. Exp. Clin. Cancer Res. 28, 82.

Ma, L., 2016. MicroRNA and metastasis. Adv. Cancer Res. 132, 165–207.

Ma, L., Young, J., Prabhala, H., Pan, E., Mestdagh, P., Muth, D., Teruya-Feldstein, J., Reinhardt, F., Onder, T.T., Valastyan, S., Westermann, F., Speleman, F., Vandesompele, J., Weinberg, R.A., 2010. miR-9, a MYC/MYCN-activated microRNA, regulates E-cadherin and cancer metastasis. Nat. Cell Biol. 12, 247–256.

Mascaux, C., Laes, J.F., Anthoine, G., Haller, A., Ninane, V., Burny, A., Sculier, J.P., 2009. Evolution of microRNA expression during human bronchial squamous carcinogenesis. Eur. Respir. J. 33, 352–359.

Nistico, P., Bissell, M.J., Radisky, D.C., 2012. Epithelial-mesenchymal transition: general principles and pathological relevance with special emphasis on the role of matrix metalloproteinases. Cold Spring Harb. Perspect. Biol. 4.

Onder, T.T., Gupta, P.B., Mani, S.A., Yang, J., Lander, E.S., Weinberg, R.A., 2008. Loss of E-cadherin promotes metastasis via multiple downstream transcriptional pathways. Cancer Res. 68, 3645–3654.

Petrova, Y.I., Schecterson, L., Gumbiner, B.M., 2016. Roles for E-cadherin cell surface regulation in cancer. Mol. Biol. Cell 27, 3233–3244.

Qi, Y., Wang, N., He, Y., Zhang, J., Zou, H., Zhang, W., Gu, W., Huang, Y., Lian, X., Hu, J., Zhao, J., Cui, X., Pang, L., Li, F., 2017. Transforming growth factor-beta1 signaling promotes epithelial-mesenchymal transition-like phenomena, cell motility, and cell invasion in synovial sarcoma cells. PLoS One 12, e0182680.

Saito, T., Oda, Y., Kawaguchi, K., Sugimachi, K., Yamamoto, H., Tateishi, N., Tanaka, K., Matsuda, S., Iwamoto, Y., Ladanyi, M., Tsuneyoshi, M., 2004. E-cadherin mutation and Snail overexpression as alternative mechanisms of E-cadherin inactivation in synovial sarcoma. Oncogene 23, 8629–8638.

Sarver, A.L., Li, L., Subramanian, S., 2010. MicroRNA miR-183 functions as an oncogene by targeting the transcription factor EGR1 and promoting tumor cell migration. Cancer Res. 70, 9570–9580.

Seoane, J., Gomis, R.R., 2017. TGF-beta family signaling in tumor suppression and Cancer progression. Cold Spring Harb. Perspect. Biol. 9.

Sheng, W., Chen, C., Dong, M., Wang, G., Zhou, J., Song, H., Li, Y., Zhang, J., Ding, S., 2017. Calreticulin promotes EGF-induced EMT in pancreatic cancer cells via Integrin/EGFR-ERK/MAPK signaling pathway. Cell Death Dis. 8, e3147.

Stacchiotti, S., Van Tine, B.A., 2018. Synovial sarcoma: current concepts and future perspectives. J. Clin. Oncol. 36, 180–187.

Su, J., Zhang, A., Shi, Z., Ma, F., Pu, P., Wang, T., Zhang, J., Kang, C., Zhang, Q., 2012. MicroRNA-200a suppresses the Wnt/beta-catenin signaling pathway by interacting with beta-catenin. Int. J. Oncol. 40, 1162–1170.

Tang, Y., Tang, Y., Cheng, Y.S., 2017. miR-34a inhibits pancreatic cancer progression through Snail1-mediated epithelial-mesenchymal transition and the Notch signaling pathway. Sci. Rep. U. K. 7.

Wicki, A., Christofori, G., 2016. E-cadherin. In: Schwab, M. (Ed.), Encyclopedia of Cancer. Springer, Berlin Heidelberg, Berlin, Heidelberg, pp. 1–5.

Xiong, K., Shao, L.H., Zhang, H.Q., Jin, L., Wei, W., Dong, Z., Zhu, Y.Q., Wu, N., Jin, S.Z., Xue, L.X., 2018. MicroRNA-9 functions as a tumor suppressor and enhances radiosensitivity in radio-resistant A549 cells by targeting neuropilin 1. Oncol. Lett. 15, 2863–2870.

Yanaihara, N., Noguchi, Y., Saito, M., Takenaka, M., Takakura, S., Yamada, K., Okamoto, A., 2016. MicroRNA gene expression signature driven by miR-9 overexpression in ovarian clear cell carcinoma. PLoS One 11, e0162584.

Yu, P.Y., Balkhi, M.Y., Ladner, K.J., Alder, H., Yu, L., Mo, X., Kraybill, W.G., Guttridge, D.C., Iwenofu, O.H., 2016. A selective screening platform reveals unique global expression patterns of microRNAs in a cohort of human soft-tissue sarcomas. Lab. Invest. 96, 481–491.

Zeisberg, M., Neilson, E.G., 2009. Biomarkers for epithelial-mesenchymal transitions. J. Clin. Invest. 119, 1429–1437.

Zhang, J., Tian, X.J., Xing, J., 2016. Signal transduction pathways of EMT induced by TGF-beta, SHH, and WNT and their crosstalks. J. Clin. Med. 5.